Supporting Information

Scalable Dry Processing of Binder-free Lithium-ion Battery Electrodes Enabled by Holey Graphene

Dylan J. Kirsch[†,ǁ], *Steven D. Lacey*[†,ǁ], *Yudi Kuang*[†], *Glenn Pastel*[†], *Hua Xie*[†], *John W. Connell*[‡], *Yi Lin**[,§], *Liangbing Hu**[,†]

† Department of Materials Science and Engineering, University of Maryland, College Park, Maryland, 20742

‡ Advanced Materials and Processing Branch, NASA Langley Research Center, Hampton, VA 23861

§ National Institute of Aerospace, Hampton, VA 23666

Corresponding Authors

* Liangbing Hu (binghu@umd.edu). * Yi Lin (yi.lin-1@nasa.gov)

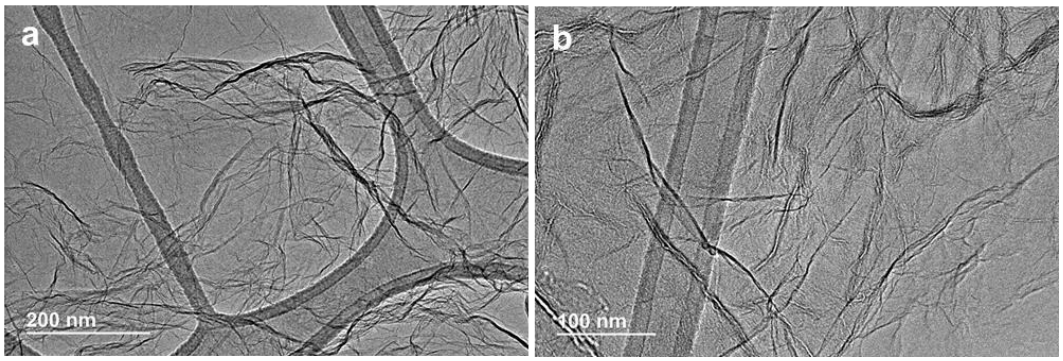

Figure S1. **(a,b)** TEM images of the micron-sized flakes of the G powder.

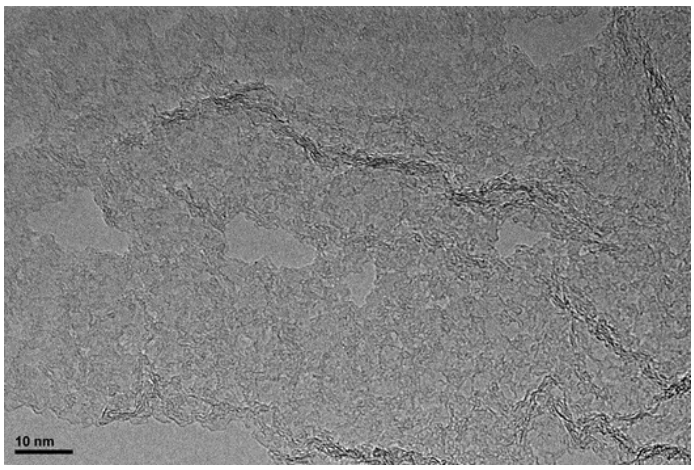

Figure S2. Zoom-in TEM image of the hG flakes showing the through-thickness holes.

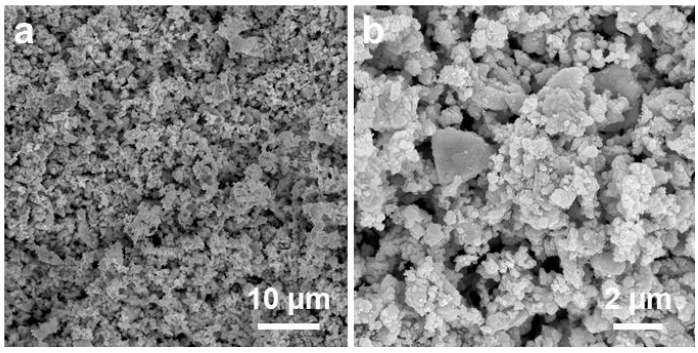

Figure S3. **(a,b)** SEM images of the commercial (carbon-coated) LFP powder with characteristic particle diameters on the order of tens to hundreds of nanometers.

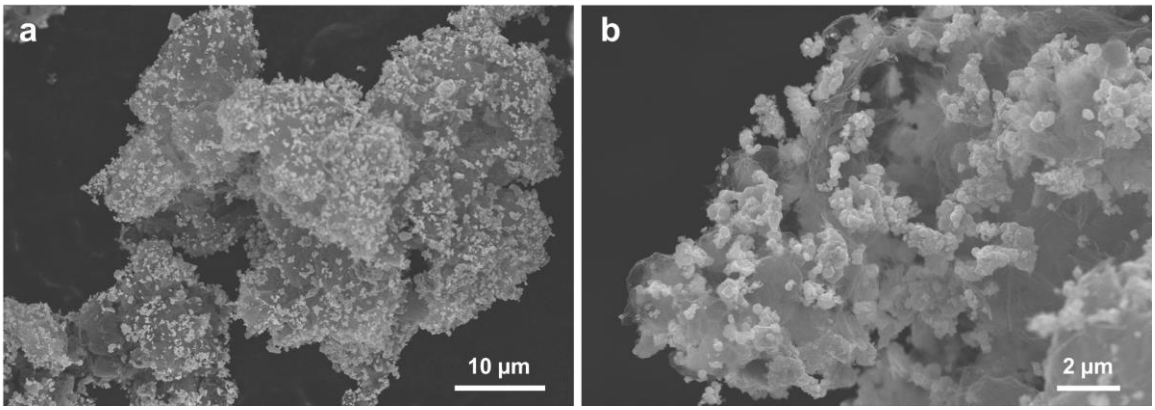

Figure S4. **(a, b)** SEM images of the mixed hG and LFP powders at different magnifications showing LFP uniformly distributed on the hG flake surface.

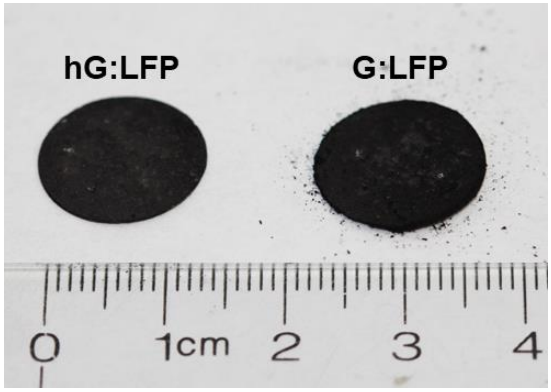

Figure S5. Digital image of dry pressed electrodes fabricated at 500 MPa using commercial LFP powder combined with (left) compressible, nanoporous hG and (right) the precursor G powder in a 1:1 weight ratio.

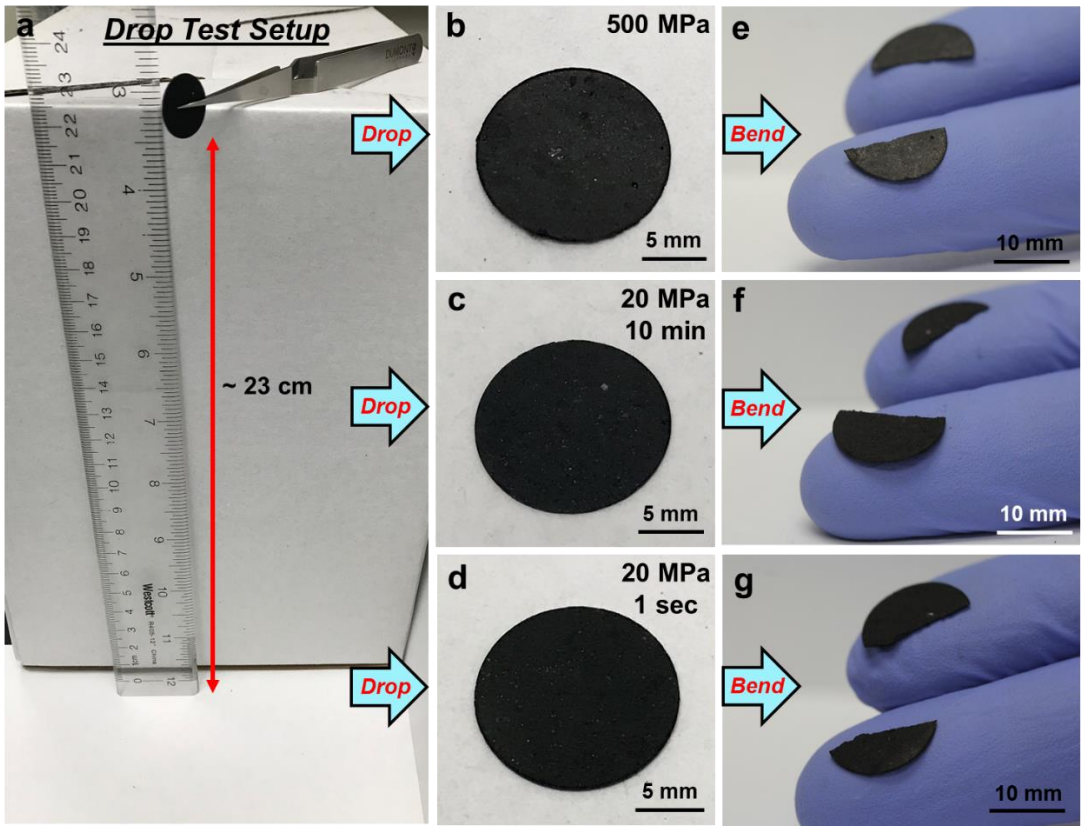

Figure S6. (a) Digital image showing the setup for the dry pressed electrode drop test, where the electrodes are dropped from a height of approximately 20 cm. Digital images of electrodes fabricated at **(b)** 500 MPa and **(c)** 20 MPa using the standard 10 minute pressing as well as **(d)** 20 MPa using a high-throughput pressing time of 1 second. Each electrode exhibits no visible or measurable weight loss following impact. Bend tests for the respective electrodes, which show identical brittle fracture characteristics: **(e)** 500 MPa [10 minute pressing], **(f)** 20 MPa [10 minute pressing], and **(g)** 20 MPa [1 second pressing].

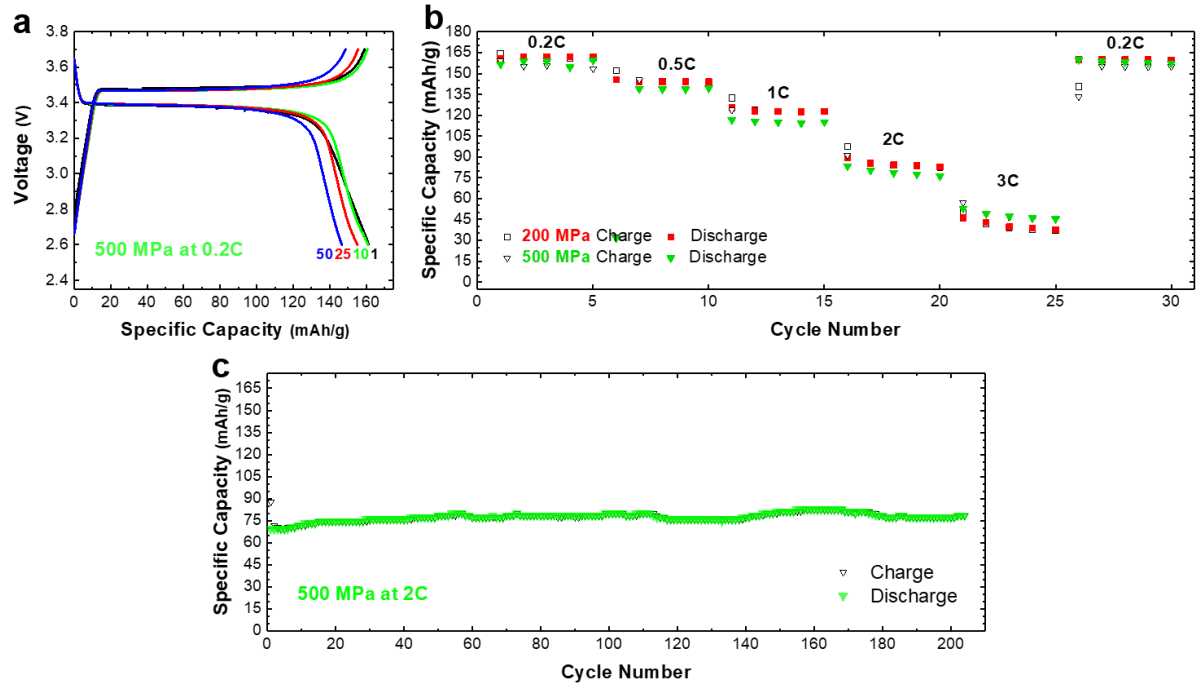

Figure S7. **(a)** Voltage profiles up to cycle 50 for a hG:LFP cathode pressed at 500 MPa cycled at 0.2C. **(b)** Rate performance of the dry pressed hG:LFP cathodes pressed at 200 (red and black squares) and 500 MPa (green and black triangles) from 0.2C to 10C. **(c)** 2C cycling performance of a 500 MPa hG:LFP cathode.

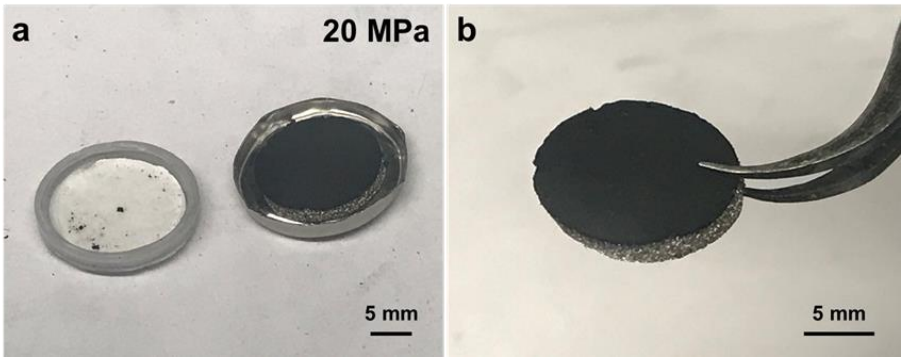

Figure S8. (a, b) Digital images of a disassembled half-cell containing a hG:LFP cathode fabricated using the lower pressing limit of 20 MPa. Notably, the dry pressed electrode maintains its robustness even after electrolyte wetting and electrochemical cycling.

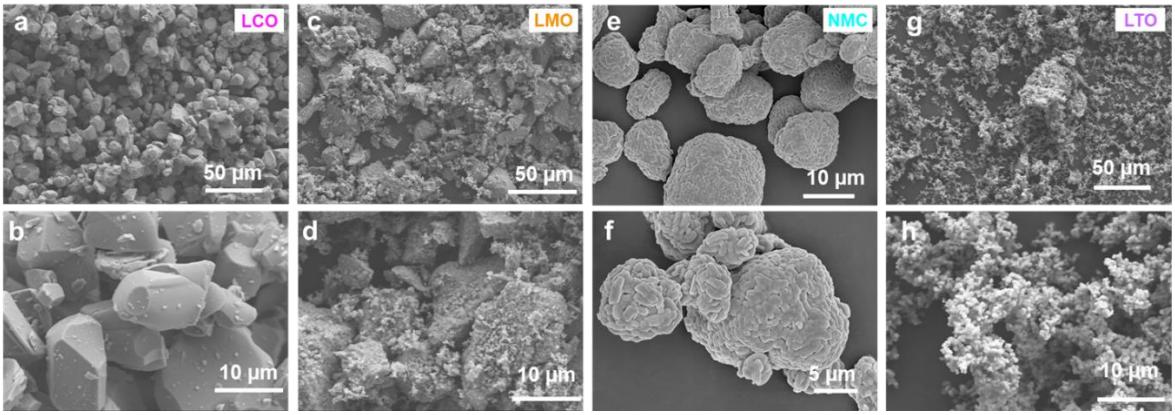

Figure S9. SEM images of each commercial LIB active material: (a,b) LCO, (c,d) LMO, (e,f) NMC, (g,h) LTO, respectively.

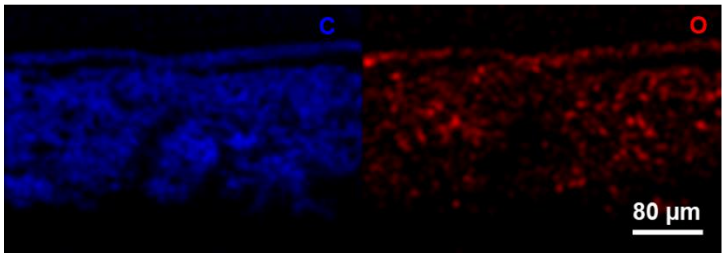

Figure S10. Cross-section EDS maps for carbon (blue) and oxygen (oxygen) for the NMC:hG composite electrode fabricated at 500 MPa.

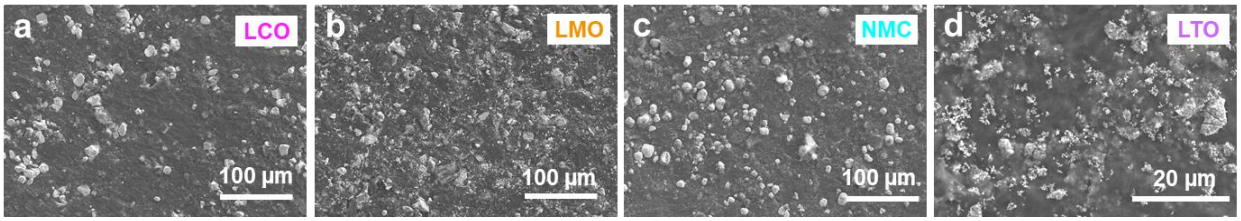

Figure S11. Top-view SEM images of dry processed composite electrodes with hG and (a) LCO, (b) LMO, (c) NMC, or (d) LTO powder, respectively, exhibiting homogeneous distribution of active material throughout.

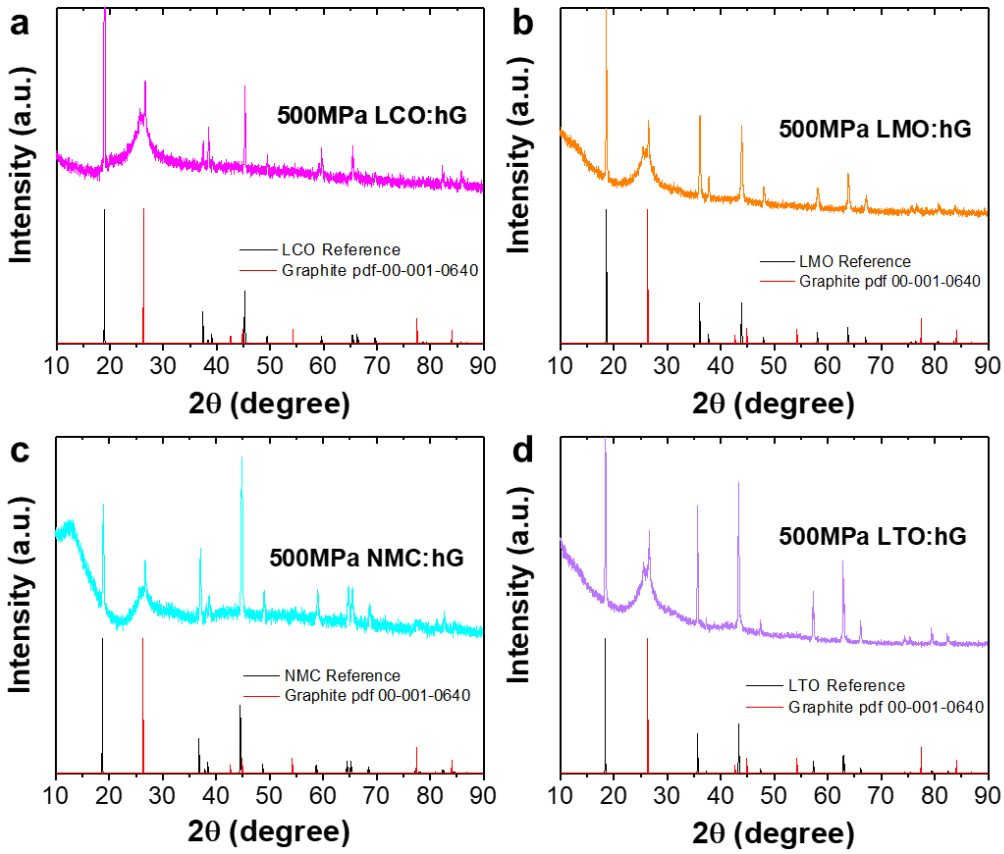

Figure S12. XRD patterns of composite LIB electrodes with **(a)** LCO, **(b)** LMO, **(c)** NMC, and **(d)** LTO, respectively. No structural changes are induced after pressing each LIB electrode at 500 MPa.